9th Asia-Pacific Conference on Wind Engineering
Auckland, New Zealand
3-7 December 2017

2D URANS Simulations of a Static Twin Box Deck: Gap Width Effect on Force Coefficients and Strouhal Number

A.J. Alvarez[1], F. Nieto[1], K.C.S. Kwok[2] and S. Hernandez[1]

[1]Structual Mechanics Research Group
University of A Coruña, Campus de Elviña s/n, 15071 A Coruña, Spain

[2]Centre for Infrastructure Engineering
Western Sydney University, Penrith (Kingswood) 2751, Australia

Abstract

The improved performance against flutter of multiple box deck configurations has increased their use in recent long span bridges projects. However, these bridges are in some cases prone to suffer from vortex induced vibration (VIV). In the present paper, the effect of gap width and angle of attack on the force coefficients and Strouhal number, has been studied by means of a 2D URANS approach. The CFD results have been compared with experimental ones, with the CFD results quite similar to the experimental ones. Two behavioural zones have been identified depending on the gap to width ratio.

Introduction

Due to its good performance against flutter, multiple box deck configurations for long-span bridges have been widely used in recent years [5]. Examples of such configurations are the cable-stayed Stonecutters Bridge, the Xihoumen Suspension Bridge, and the Messina Strait Bridge project.

On the other hand, the flow around the decks of this type of configuration is more complex and the bridges are more susceptible to suffer vortex induced vibrations (VIV). For this reason, a wide range of experimental campaigns have been carried out ([2], [6], [3]) in order to assess the behaviour of these configurations, and the dependency on the gap distance between decks. These setups require expensive facilities and many hours of preparation and testing. In contrast, relatively inexpensive 2D URANS can provide a feasible alternative for the qualitative study of this deck typology.

It is the goal of this work to conduct 2D Unsteady Reynolds-Averaged Navier-Stokes (URANS) simulations to study the effect of the gap width on the force coefficients, mean and standard deviation distributions of pressure coefficients, and vortex shedding phenomenon. A bare twin box deck arrangement with geometry similar to the Stonecutters Bridge has been chosen as an application case. The range of investigated gap to depth ratios, G/D is (0, 9.7) and the interval of considered angle of attack is (-10°, 10°).

Formulation

Governing Equations

The flow around bodies is modelled by the Navier-Stokes equations, whose time averaging in conservative form yields the Unsteady Reynolds-Averaged Navier-Stokes (URANS) [10] equations:

$$\frac{\partial U_i}{\partial x_i} = 0 \qquad (1)$$

$$\rho\frac{\partial U_i}{\partial t} + \rho U_i\frac{\partial U_i}{\partial x_j} = -\frac{\partial P}{\partial x_i} + \frac{\partial}{\partial x_j}\left(2\mu S_{ij} - \rho\overline{u_i' u_j'}\right) \qquad (2)$$

Where U_i is the i-esime component of the mean velocity vector, x_i is the i-esime component of the position vector, ρ is the fluid density, t is the time, P is the mean pressure, μ is the fluid viscosity, S_{ij} are the components of the mean strain-rate tensor and u_i' is the i-esime component of the fluctuating velocity vector. The term $-\rho\overline{u_i' u_j'}$ is the so-called specific Reynolds stress tensor (τ_{ij}), calculated by means of the Boussinesq assumption as:

$$\tau_{ij} = 2\upsilon_T S_{ij} - \frac{2}{3}k\delta_{ij} \qquad (3)$$

Where υ_T is the kinematic eddy viscosity and k is the kinetic energy per unit mass of the turbulent fluctuation.

Depending on the equations added for the closure of the system, different URANS models are obtained. In this case, the $k-\omega$ SST turbulence model, for incompressible flow implemented in the open source software OpenFOAM [8], has been used.

Force Coefficients and Strouhal Number

The force coefficients and Strouhal number (S_t), are calculated as indicated in the following equations. Positive lift and moment are the upward direction and the clockwise rotation respectively. Positive drag is taken in the alongwind direction, which is coincident with the positive x-axis as shown in Figure 1.

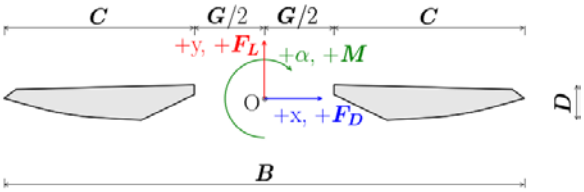

Figure 1: Sign convention.

$$C_d = \frac{F_D}{\frac{1}{2}\rho U^2 C}; C_l = \frac{F_L}{\frac{1}{2}\rho U^2 C}; C_m = \frac{M}{\frac{1}{2}\rho U^2 C^2}; S_t = \frac{fD}{U} \qquad (4)$$

Grid discretization strategy, verification and validation

The geometry considered for the verification and validation studies is the one identified as Gap 4 in [2], which closely corresponds to the actual Stonecutters Bridge. In the simulations, the model geometric scale is 1:80, sharp edges were considered and no guide vanes were included, as specified in the aforementioned reference.

The overall size of the computational domain is shown in Figure 2, which is similar to the one reported in [1]. The computational domain has been divided in three different zones, without considering the boundary layer regions. The zone closest to the

Mesh	y_1/C	x_1/y_1	r	l_{bl}	y_{bl}/C	Total cells	Quadrilateral cells	Triangular cells
coarse	$1.6432 \cdot 10^{-4}$	4	1.167	10	$3.5035 \cdot 10^{-3}$	413118	66820	42250
medium	$1.6432 \cdot 10^{-4}$	4	1.167	10	$3.5035 \cdot 10^{-3}$	664032	66820	597212
fine	$1.6432 \cdot 10^{-4}$	2	1.167	10	$2.3808 \cdot 10^{-3}$	1359262	133260	1226002

Table 1: Mesh properties. The parameter y_1 is the total height of the first element of the boundary layer (bl), x_1 is the length of first element in the bl, r is the growth ratio of the elements in the bl, l_{bl} is the number of layers forming the bl and y_{bl} is the total height of the bl.

decks is the so called buffer zone (L), where special care was taken to obtain a high density mesh in the gap between decks. A narrow strip is defined downstream of the buffer zone, which is the wake zone (M). Finally, further away from the decks, the zone (N) is defined, where the coarsest elements are placed. In the figure, *C* is the width of one deck, *G* the gap between decks, *B* the overall width of the decks, and D the height.

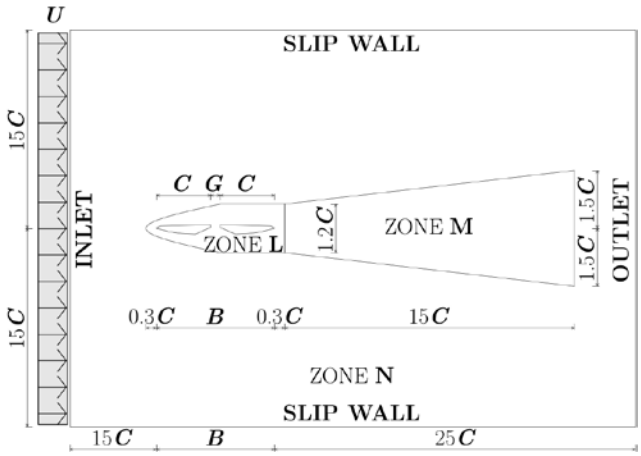

Figure 2: Computational domain.

In CFD simulations, the finite volume mesh discretization of the computational domain plays a key role in the validation of the results [7]. Therefore a mesh density sensitivity study was carried out. This process tries to identify a mesh in which successive spatial refinements do not produce significant changes in the numerical results. Three meshes, with different densities, have been considered. Their properties can be found in Table 1. All the simulations in this study were carried out at $Re = U_\infty D/\nu = 4.48 \cdot 10^4$, corresponding to a wind speed of 15m/s, for a zero degree angle of attack (α = 0°).

It must be kept in mind that the high number of elements of the meshes is related to the complexity of the geometry studied, in shape and in number of decks, since the downstream one is fully immersed in the wake of the upstream box.

The type of mesh employed was a triangular non-structured mesh, except for the boundary layer region, where a quadrangular structured mesh was used. The differences between meshes mainly reflect the successive refinement of the different zones, keeping the same discretization for the boundary layer except for the fine mesh, where the length of the elements in the first layer attached to the twin boxes is half the length adopted in the other meshes. The height of the boundary layer first element has been chosen in order to get a non-dimensional first layer height target value of two ($y^+ = (u_\tau y_1)/\nu$; y_1 is the total height of the first element of the boundary layer and u_τ is the friction velocity). The characteristics of the three different meshes considered in the verification study are summarized in Table 1, while the results of the grid sensitivity study are presented in Table 2.

Mesh	C_d	C_l	C_m	C'_d	C'_l	C'_m	S_t
coarse	0.143	-0.264	0.021	0.05	0.43	0.12	0.26
medium	0.146	-0.232	0.028	0.06	0.52	0.11	0.28
fine	0.144	-0.238	0.023	0.06	0.52	0.11	0.28

Table 2: Results of the grid-refinement study.

The values of the y^+ obtained for the left and right boxes are similar to the ones reported in [9]. In all cases the percentage of elements with $y^+ > 4$ is lower than 1.5% and the average value is lower than 2. The maximum values are mainly located in the vicinity of the deck corners.

All the previous results have been computed imposing a maximum Courant number (*Co*) of 10. This number was selected due to the high number of elements in the mesh and its high computational cost, in order to reduce the computational time of the simulations. As the time discretization can affect the results, a sensitivity study imposing different maximum values of *Co* was also carried out.

The values obtained from the statistical treatment of the time-histories of the force coefficients at different maximum *Co*, are presented in Table 3. No major differences have been found between the different simulations apart from some reductions in the standard deviation of the lift coefficient, related to the variations present in the distribution of the pressure coefficient standard deviation (C'_p) that are explained next.

Co	C_d	C_l	C_m	C'_d	C'_l	C'_m	S_t
10	0.146	-0.232	0.028	0.06	0.52	0.11	0.28
5	0.142	-0.240	-0.001	0.06	0.45	0.12	0.27
1	0.142	-0.241	-0.044	0.05	0.41	0.12	0.26

Table 3: Results for different *Co* numbers.

In Figure 3, the mean and standard deviation distributions of the pressure coefficient are reported for the Gap04 case. ($C_p = (p - p_0)/[(1/2)\rho U_\infty^2]$; p is the local pressure, p_0 is the far upstream pressure, ρ is the air density and $U_\infty$is the free stream speed)

Focusing firstly on the differences obtained for the numerical simulations conducted for different mesh densities and time discretization, it can be shown that the differences in the mean pressure distribution are negligible once the coarse mesh is discarded. On the other hand, for the simulations conducted with imposed lower maximum Co, some small differences in the pressure coefficient standard deviation distribution in the downwind box are apparent. The time step refinement produces a small decrement in the pressure standard deviation in the regions where the vortices shed from the windward box impinge on the downwind one. In Table 3, it can be appreciated how the standard deviation of the lift coefficient (C'_l) slightly diminishes as the maximum Co is reduced. Bearing in mind the goals of these simulations (analyses of mean force coefficients and S_t for a wide range of deck gaps) and the high computational burden associated with a 10 times lower maximum *Co* (Co^{max} =1), the medium mesh characteristics and a maximum *Co* of 10 are retained for the other gap to depth ratios considered hereafter.

Focusing now on the consistency of the numerical results with the wind tunnel data, in Figure 3 the mean pressure distribution around the upwind box obtained in the wind tunnel is very similar to the CFD results. On the other hand, for the mean pressure distribution around the downwind box, some discrepancies can be found between experimental and numerical results. In the upper side, close to the windward corner, and in the curved plate in the lower side, higher pressure coefficients are obtained in the CFD simulations. These differences do not have an impact in the mean force coefficients obtained in the numerical simulations when they are compared with the wind tunnel data. In fact, the distance from

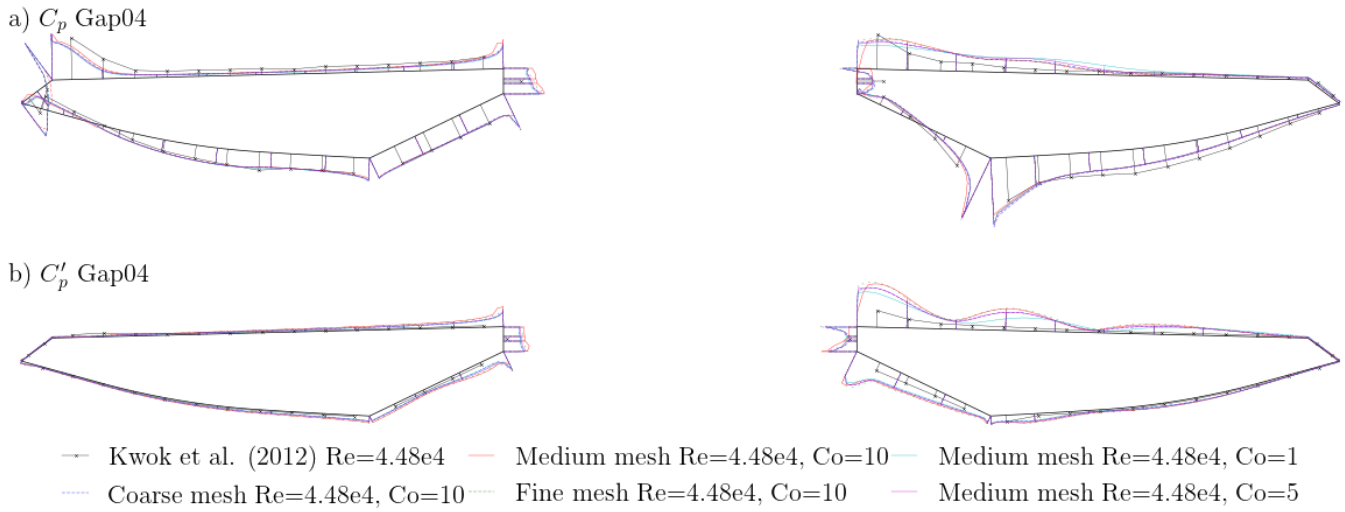

Figure 3: Mean pressure coefficient distribution and its standard deviation distribution. Negative values points outward the section and the height of the section is equal to a value of unity.

the centre of pressures in the downwind box to point O (Figure 1) amplifies the discrepancies in the value of moment coefficient. The differences in the standard deviation of the pressure coefficient on the upper side of the downwind box between experimental and numerical data, are related to the strong vortices typical of two equation turbulence models and the inability of 2D URANS models to simulate the correlation characteristics of the real 3D case flow.

It must be highlighted that, to the knowledge of the authors, no previous studies of multi-box decks have reported a mesh and a time discretization sensitivity study like the one reported herein.

The force coefficients and Strouhal number (S_t) obtained for the Gap04 case are presented in Table 4. The results are in good agreement with the experimental results, and the only discrepancy can be found in the C_m, which can be explained by the amplification of the minor errors associated with the distribution of the mean pressure coefficient in the downstream deck, as it was previously mentioned.

In the experimental value of S_t presented Table 4, the deck depth is *D*=3.609m which is the value reported in [4], instead of *D*=3.5m in [2].

Results

Simulations have been conducted for 14 different gap distances, and for different angles of attack. Values of the force coefficients for 11 different angles of attack for Gap04 are shown in Figure 4, whilst in Figure 5 the values of the force coefficients for all the gap widths studied at $\propto = 0°$ are presented.

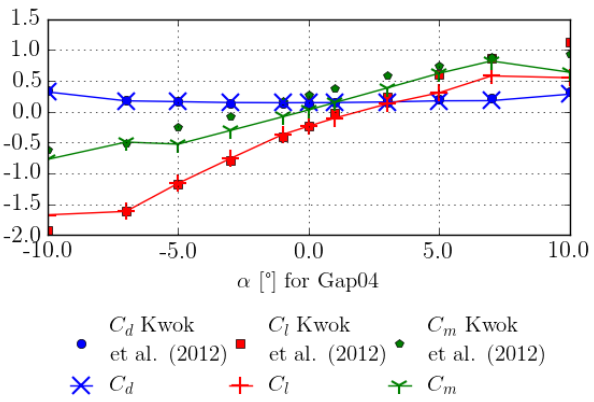

Figure 4: Force coefficients for Gap 04.

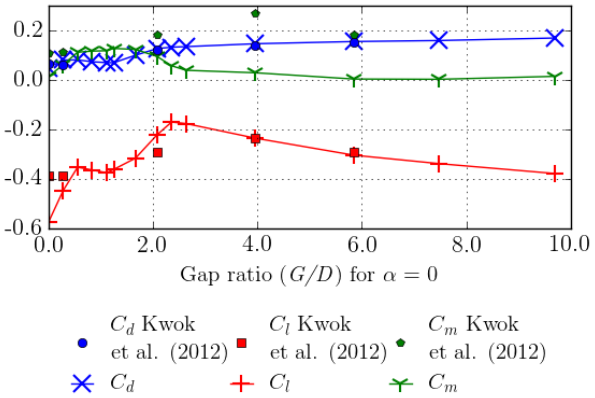

Figure 5: Force coefficients for different gap ratios at $\alpha = 0$..

The S_t values for the different gaps studied are presented in Figure 6.

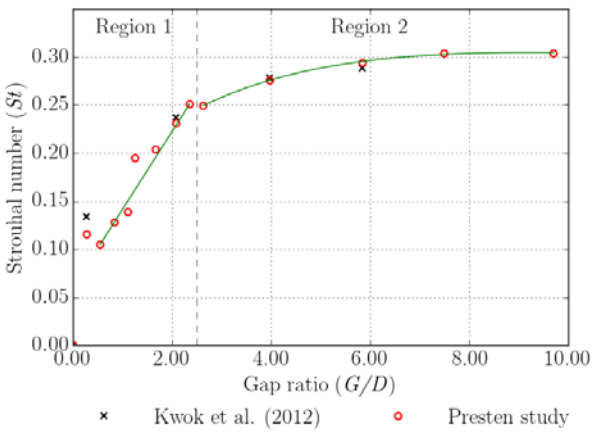

Figure 6: Strouhal number (S_t) for different gap ratios.

It can be seen that the values are in good agreement with the experimental ones reported by [2]. Moreover, two different behavioural zones are identified as in the case of [3]. In the first zone the S_t value increases linearly with the gap ratio and vortices are shed from both decks. On the other hand, a second region where the change in the S_t follows a parabolic trend was identified from G/D = 2.49. In this region, vortices are mainly shed from the upstream deck and travel along the downstream deck. As the

	Method	Re	I[%]	C_d	C_l	C_m	C'_d	C'_l	C'_m	S_t
Present study	$k-\omega$ SST	$4.48 \cdot 10^4$	1.0	0.146	-0.232	0.028	0.058	0.521	0.108	0.278
Kwok et al. (2012	Exp.	$4.48 \cdot 10^4$	-	0.140	-0.234	0.267	-	-	-	0.278

Table 4: Comparison between experimental and numerical values. All data calculated respect *C* except for S_t calculated respect *D*.

distance between decks grows, the interaction between decks diminishes, which corresponds with the asymptotic trend in the second zone. Finally, if the decks are placed far enough their behaviour is completely independent.

Conclusions

During the design of a twin box section bridge, the gap between decks plays a major role in its aerodynamic behaviour. Therefore relatively inexpensive 2D URANS simulations can help assessing the effect caused by the gap distance in the force coefficients. 2D URANS has also been proven to be capable of predicting satisfactorily the vortex shedding response of this type of sections.

Acknowledgments

This research has been funded by the Spanish Ministry of Economy and Competitiveness in the frame of the research project with reference BIA2016-76656-R and the Galician regional goverment (including FEDER Funding) with reference GRC2013-056. One of the authors has been funded by the Spanish Ministry of Economy and Competitiveness (including ESF funding) in the frame of the National Program for Promotion of Talent and Employability through the BES-2014-068418 pre-doctoral contract grant, associated with the BIA2013-41965-P research project.

The computations have been carried out in the computer cluster Breogan and in the Galician Supercomputation Technology Centre (CESGA).

The authors fully acknowledge the received support.

References

[1] Bruno, L., Fransos, D., Coste, N. and Bosco, A., 3D flow around a rectangular cylinder: A computational study, *Journal of Wind Engineering and Industrial Aerodynamics*, **98**, 2010, 263–276.

[2] Kwok, K., Qin, X., Fok, C. and Hitchcock, P., Windinduced pressures around a sectional twin-deck bridge model: Effects of gap-width on the aerodynamic forces and vortex shedding mechanisms, *Journal of Wind Engineering and Industrial Aerodynamics*, **110**, 2012, 50–61.

[3] Laima, S. and Li, H., Effects of gap width on flow motions around twin-box girders and vortex-induced vibrations, *Journal of Wind Engineering and Industrial Aerodynamics*, **139**, 2015, 37–49.

[4] Larose, G., Larsen, S., Larsen, A., Hui, M. and Jensen, A., Sectional model experiments at high Reynolds number for the deck of a 1018 m span cable-stayed bridge, *in Proceedings of The Eleventh International Conference on Wind Engineering*, Lubbock, Texas, USA, 2003.

[5] Larsen, A. and Walther, J., Aeroelastic analysis of bridge girder sections based on discrete vortex simulations, *Journal of Wind Engineering and Industrial Aerodynamics*, **67-68**, 1997, 253–265.

[6] Li, H., Laima, S. and Jing, H., Reynolds number effects on aerodynamic characteristics and vortex-induced vibration of a twin-box girder, *Journal of Fluids and Structures*, **50**, 2014, 358–375.

[7] Mannini, C., Soda, A. and Schewe, G., Unsteady RANS modelling of flow past a rectangular cylinder: Investigation of Reynolds number effects, *Computers & Fluids*, **39**, 2010, 1609–1624.

[8] Menter, F. and Esck, T., Elements of Industrial Heat Transfer Prediction, in *Proceedings of the 16th Brazilian Congress of Mechanical Engineering*, 2001, volume 20, 117–127, 117–127.

[9] Nieto, F., Owen, J., Hargreaves, D. and Hernandez, S., Bridge deck flutter derivatives: Efficient numerical evaluation exploiting their interdependence, *Journal of Wind Engineering and Industrial Aerodynamics*, **136**, 2015, 138–150.

[10] Wilcox, D., *Turbulence Modelling for CFD*, DCW Industries, La Cañada, 2006, third edition.